Bulletin of Electrical Engineering and Informatics
Vol. 12, No. 5, October 2023, pp. 2693∼2704
ISSN: 2302-9285, DOI: 10.11591/eei.v12i5.5014

Induction motor performance improvement using a five-level inverter topology and sliding mode controllers

Chaymae Fahassa[1], Ahmed Abbou[1], Yassine Zahraoui[2], Mohamed Akherraz[1]
[1]Department of Electrical Engineering, Laboratory of Power Electronics and Control, Mohammadia School of Engineers (EMI), Mohammed V University, Rabat, Morocco
[2]Department of Electrical Engineering, Higher National School of Arts and Crafts (ENSAM), Hassan II University, Casablanca, Morocco

Article Info

Article history:

Received Oct 15, 2022
Revised Nov 2, 2022
Accepted Dec 22, 2022

Keywords:

Five-level NPC inverter
Induction motor drive
Performance improvement
Sliding mode controllers
Vector control scheme

ABSTRACT

This research intends to establish a robust vector control (VC) of a 3-ϕ induction motor (IM). The classical 2-level inverter is displaced by a 5-level neutral-point-clamped (NPC) inverter. The 2-level inverter may only supply 8 voltage vectors, while the 5-level NPC inverter can furnish 125 voltage vectors. The objective is to bring about a command voltage vector that converges to the reference voltage vector as closely as possible; hence, guaranteeing a quick response on one hand and improving the dynamic performance on the other hand. A robust sliding mode controller (SMC) structure is used in all regulation loops. Satisfactory results are obtained for various speed zones. The quality and robustness of the global system are tested under resistive torque disturbance, reversal, high, and low-speed ranges in order to prove system stability. All the simulations have been performed under MATLAB/Simulink.

Corresponding Author:

Chaymae Fahassa
Laboratory of Power Electronics and Control, Department of Electrical Engineering
Mohammadia School of Engineers (EMI), Mohammed V University
Rabat, Morocco
Email: fahassa.chaymae@gmail.com

1. INTRODUCTION

Towards the middle of the 1970s, a new concept of induction machine control, called vector control (VC) or field-oriented control (FOC) appeared to be competitive with other control techniques, especially scalar control (SC) [1]. Unlike the last, which is based on pointed but strict mathematical formalisms, VC schemes were initially based on qualitative and clarified knowledge of the conduct of the machine [2]. Often tuning actions were taken on using classical PI controllers and pulse width modulators (PWM). The implementation of these algorithms was therefore simpler, at a time when computing resources were constantly improving in power and speed [3].

The decisive advantages attributed to conventional VC techniques (dynamics, robustness, ease of implementation, performance at low speeds) [4] are nevertheless counterbalanced by the use of a sampled hysteresis or PI regulators; in theory, the regulator drives to a variable frequency action which increases the risks of excitation of mechanical or acoustic resonances [5], and on the other hand, limit frequency sampling outcomes in a pseudo-random exceed of the hysteresis strip. These two factors contribute to making the harmonic content of the various output signals difficult to predict [6]. Simultaneously, new and promising static conversion topologies, called multilevel, have been proposed and increasingly used in high-power variable speed drive applications [7]. Compared to conventional two-level structures, in which the output voltage can only be modulated by acting on the duration of use of the high state and the low state, pulse width modulation, multilevel structures indeed open up a new dimension, it's the amplitude modulation [8], [9].

In the present study, our main objective is to propose new strategies of the VC type, compatible with multilevel voltage inverters (more particularly multicellular), having any number of levels. Their application to conventional two-level inverters will only be seen as a special case [10]. We will endeavor to show that a control judiciously exploiting the degrees of freedom offered by these new conversion structures allows to minimize the drawbacks of conventional VC strategies while retaining their advantages [11].

The principal aim of this research is to enhance the performance of the VC applied to the induction machine. We propose a control plan established on nonlinear sliding mode controller (SMC) [12], [13] (without the use of hysteresis or PI controllers) and a five-level neutral point clamped (NPC) inverter in order to obtain an optimal voltage control allowing the best choice of the sequence of the voltage vector to be carried out to the machine while respecting the constraints on the flux and the electromagnetic torque. This will produce a robust VC scheme without resorting to the conventional PI controllers used in the classical VC scheme [14], [15].

2. IM STATE-SPACE MATHEMATICAL MODEL

The state-space modeling representation of an IM could be mathematically written as:

$$\begin{cases} \dot{X} = \mathbf{A_1}X + \mathbf{B_1}U \\ Y = \mathbf{C_1}X \end{cases} \tag{1}$$

The state vector was represented as X, the input as U, and the output as Y. As stated by [16], the state and the input vectors of an IM can be specified by the stator current and the rotor flux components based on their rotational d-q frame. Thus, they can be defined as: X=$[I_{s_d} \quad I_{s_q} \quad \Phi_{r_d} \quad \Phi_{r_q}]^t$, U=$[V_{s_d} \quad V_{s_q}]^t$, and Y=$[I_{s_d} \quad I_{s_q}]^t$. I_{s_d} and I_{s_q} are components of the stator current in the d-q reference axes. Φ_{r_d} and Φ_{r_q} are components of the rotor flux. V_{s_d} and V_{s_q} are components of the stator voltage. Thus, components of matrices in the state-space representing could be obtained by construing differential equations of the stator currents and the rotor fluxes [17], as in the equation:

$$\mathbf{A_1} = \begin{bmatrix} -c_1 & 0 & \frac{c_2}{\tau_r} & c_2\Omega_r \\ 0 & -c_1 & -c_2\Omega_r & \frac{c_2}{\tau_r} \\ \frac{L_m}{\tau_r} & 0 & -\frac{1}{\tau_r} & -\Omega_r \\ 0 & \frac{L_m}{\tau_r} & \Omega_r & -\frac{1}{\tau_r} \end{bmatrix}; \quad \mathbf{B_1} = \begin{bmatrix} \frac{1}{\sigma L_s} & 0 \\ 0 & \frac{1}{\sigma L_s} \\ 0 & 0 \\ 0 & 0 \end{bmatrix}; \quad \mathbf{C_1} = \begin{bmatrix} 1 & 0 & 0 & 0 \\ 0 & 1 & 0 & 0 \end{bmatrix}$$

With c_1=$\frac{R_s}{\sigma L_s}$+$\frac{1-\sigma}{\sigma \tau_r}$; c_2=$\frac{1-\sigma}{\sigma L_m}$; σ=1-$\frac{L_m^2}{L_s L_r}$; τ_r=$\frac{L_r}{R_r}$. The electrical power is written as:

$$P_e = p\frac{L_m}{L_r}(\Phi_{r_d} I_{s_q} - \Phi_{r_q} I_{s_d})\Omega_r \tag{2}$$

The expression of the torque is came by dividing the electromechanical power P_e over Ω_r, whence:

$$T_e = p\frac{L_m}{L_r}(\Phi_{r_d} I_{s_q} - \Phi_{r_q} I_{s_d}) \tag{3}$$

The rotor mechanical speed is formulated by:

$$J\frac{d\Omega_r}{dt} = T_e - T_l - Fr\Omega_r \tag{4}$$

J is the inertia coefficient of the motor, T_l is the torque of the load, and Fr is the coefficient of the friction [18]. The block diagram of the state-space modeling of IM could be seen in Figure 1.

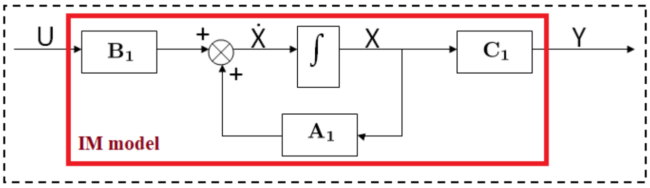

Figure 1. Mathematical model in state-space of an IM

3. VECTOR CONTROL BASIS

The direct scheme of VC demands a right acquaintance of the modulus and phase of the rotor fluxes. The basic idea is to place sensors in the motor air gap to access the flux [19]. Nevertheless, the installation of these sensors leads to a rise in the size and a weakening of the motor [20]. Moreover, these sensors are responsive to mechanical shocks and heat. Rather, gauged quantities such stator current and voltage might be used to estimate rotor fluxes [21]. The stator flux may be estimated then by an integration:

$$\hat{\Phi}_{s_{\alpha\beta}} = \int_0^t (V_{s_{\alpha\beta}} - R_s I_{s_{\alpha\beta}})dt \tag{5}$$

And the rotor fluxes might be estimated from the stator flux and the real stator current [22]:

$$\hat{\Phi}_{r_{\alpha\beta}} = \frac{L_r \hat{\Phi}_{s_{\alpha\beta}} - L_s L_r \sigma I_{s_{\alpha\beta}}}{L_m} \tag{6}$$

Subsequently, the flux norm $\hat{\Phi}_r$ and its position $\hat{\theta}_s$ utilized for coordinate transformation are determined by [23]:

$$\hat{\Phi}_r = \sqrt{\hat{\Phi}^2_{r_\alpha} + \hat{\Phi}^2_{r_\beta}} \tag{7}$$

$$\hat{\theta}_s = \arctan(\frac{\hat{\Phi}_{r_\beta}}{\hat{\Phi}_{r_\alpha}}) \tag{8}$$

4. SLIDING MODE SPEED CONTROLLER

Generally, Jean-Jacques Slotine suggested an equation way to define the sliding surface which assure variable converging to the wanted result [24]:

$$S(X) = (\frac{d}{dt} + \lambda)^{n-1} E(X) \tag{9}$$

$E(X)$=X^*-X: gap variable to be settled, λ: coefficient which is strictly positive, n: relative degree that represents the number of times to derive the output to get the appropriate control [25], [26]. By selecting (n=1) in Jean-Jacques Slotine general (9), the sliding surface of the speed is specified by:

$$S(\Omega_r) = \Omega_r^* - \Omega_r \tag{10}$$

Its derivative is:

$$\dot{S}(\Omega_r) = \dot{\Omega}_r^* - \dot{\Omega}_r = \dot{\Omega}_r^* - \eta \Phi_r I_{s_q} + \frac{T_l}{J} + \frac{Fr}{J}\Omega_r \tag{11}$$

By inserting the control current $I^*_{s_q}$=$I_{sq_{eq}}$+I_{sq_n} in (11):

$$\dot{S}(\Omega_r) = \dot{\Omega}_r^* - \eta \Phi_{r_d} I_{sq_{eq}} - \eta \Phi_r I_{sq_n} + \frac{T_l}{J} + \frac{Fr}{J}\Omega_r \tag{12}$$

Throughout the sliding mode and steady state $S(\Omega_r)$=0, $\dot{S}(\Omega_r)$=0, and I_{sq_n}=0, we next obtain the equivalent control expression $I_{sq_{eq}}$:

$$I_{sq_{eq}} = \frac{1}{\eta \phi_r}(\dot{\Omega}_r^* + \frac{T_l}{J} + \frac{f}{J}\Omega_r) \tag{13}$$

Throughout the converging mode, the discontinued control form i_{sq_n} should fulfill the condition $\dot{S}(\Omega_r)S(\Omega_r){<}0$. By substituting $I_{sq_{eq}}$ expression in (12), we obtain:

$$\dot{S}(\Omega_r) = -\eta\Phi_r I_{sq_n} \tag{14}$$

The discontinued control form is then put as:

$$I_{sq_n} = G_\Omega sat(\frac{S(\Omega_r)}{\epsilon_{\Omega_r}}) \tag{15}$$

5. FIVE-LEVEL NPC INVERTER DESIGN

The general schema of the 5-Level NPC inverter is given in Figure 2. This structure consists of 3 symmetrical arms; each arm contains 8 bi-directional switches mounted in series. These interrupters should not be opened or closed at the same instant, to avert the short-circuit of the inverter input continuous voltage [27]. Each switch is made up of a bi-controllable semiconductor S_{ij} (i=A, B, C and j=1, ..., 8) and a diode posed in anti-parallel. The number of floating diodes is 10 per arm D_k (k=1, ..., 10) ensuring the appliance of various voltage levels at each arm output [28].

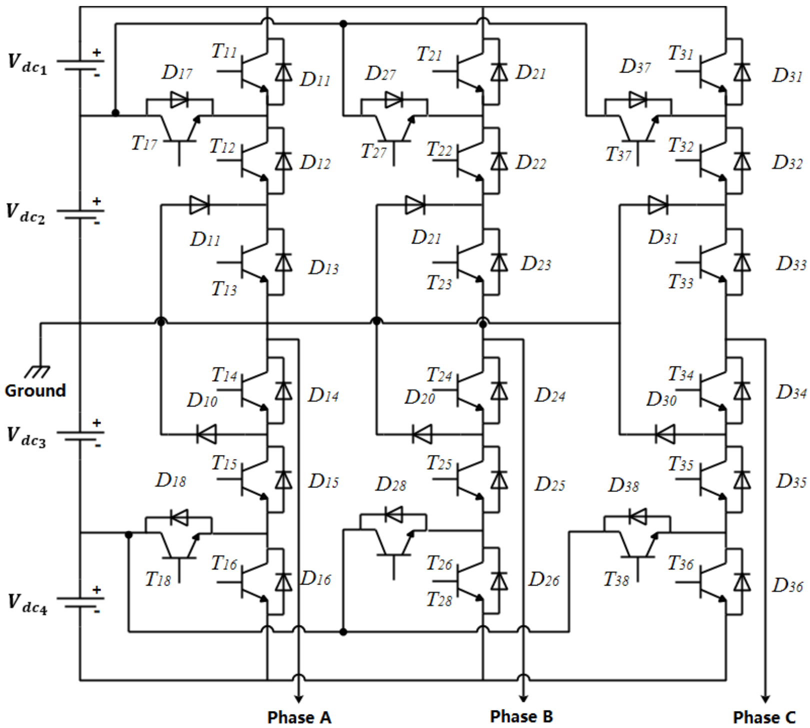

Figure 2. The schema of the five-level NPC inverter

This inverter is called a 5-level because it issues five voltage levels per arm ($+\frac{V_{dc}}{2}$, $+\frac{V_{dc}}{4}$, 0, $-\frac{V_{dc}}{4}$, $-\frac{V_{dc}}{2}$). By combining the twelve switches of the same arm, seven different voltage levels can be applied to the same phase:

$$\begin{cases} (1,1,1,1,0,0,0,0) \rightarrow +\frac{V_{dc}}{2} \\ (1,1,1,0,1,0,0,0) \rightarrow \;\; +\frac{V_{dc}}{4} \\ (1,1,0,0,1,1,0,0) \rightarrow 0 \\ (1,0,0,0,1,1,1,0) \rightarrow \;\; -\frac{V_{dc}}{4} \\ (0,0,0,0,1,1,1,1) \rightarrow -\frac{V_{dc}}{2} \end{cases} \tag{16}$$

As a result, unlike the two-level inverter, which can only issue 8 voltage vectors. The 5-level NPC inverter can give 125 voltage vectors [29].

The 125 positions of the output voltage vector separate the vector diagram into 6 triangular sectors. Each sector is made up of thirty-six triangular regions. There are thus two hundred sixteen triangular regions in the complete vector diagram. Multilevel inverters are a good choice for many system applications, especially for drive systems. This is because they provide many advantages like power factor improvement and THD reduction [30]. The block diagram of the suggested VC scheme with the SMC and the 5-level NPC inverter is illustrated in Figure 3.

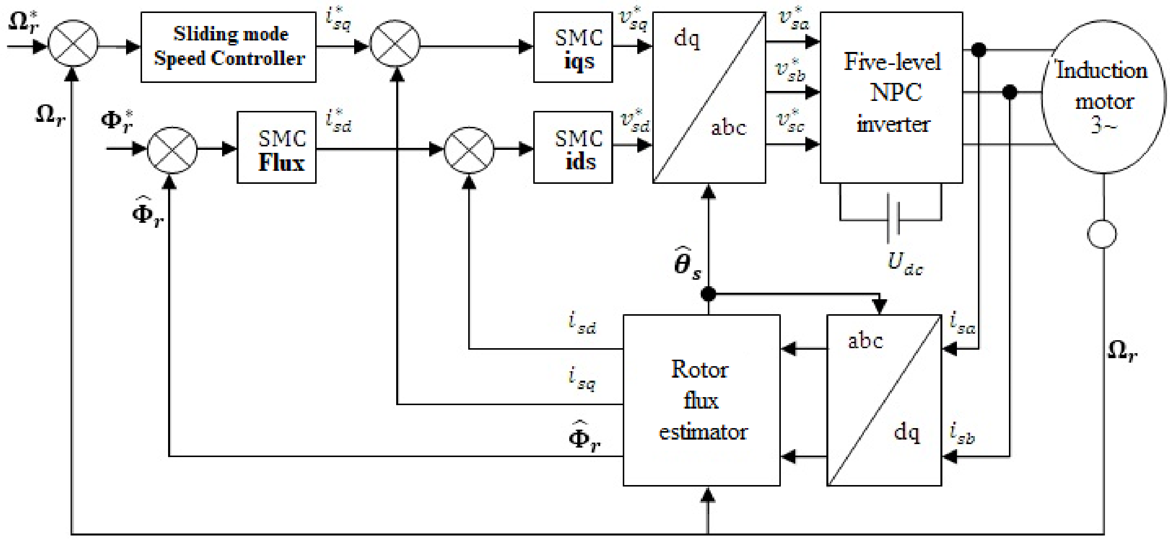

Figure 3. The control scheme of the suggested technique

6. SIMULATION RESULTS AND DISCUSSION

Figures 4-7 highlight the simulation results under a resistive disturbance. A resistive torque of +15 $N.m$ is appealed at 0.8 seconds and eliminated at 1.8 seconds. The resistive torque is expressed as T_r=Ωf_r+T_l, f_r is the coefficient of the machine viscous friction, and T_l is the torque of the load. The reference of the rotor flux is fixed to 1 Wb. The gain of the SMC regulator used in the speed loop is: G_Ω=5$\times$10^3. It is determined by trial and errors in the speed closed loop. The rated parameters of the motor used in the simulation are: rated speed: 1440 rpm, frequency: 50 Hz, pole pair number: 2, line-to-line voltage: 220/380 V, phase current: 12.5/7.2 A, stator resistance: 2.2 Ω, rotor resistance: 2.68 Ω, stator inductance: 0.229 H, rotor inductance: 0.229 H, mutual inductance: 0.217 H, moment of inertia: 0.047 $kg.m^2$, coefficient of viscous friction: 0.004 $N.s/rad$.

6.1. Results analysis

The results illustrated in Figure 4 prove good tracking of the reference speed. The speed regulation loop-based SMC reject quickly the disturbance of the applied load (Figure 4(a)). The response time is less than 0.2 seconds for a reference of +100 rad/s. Once the steady state is reached, the system no longer needs torque. The speed controller cuts the torque demand; it is never zero because it should overcome the friction of the machine which is represented by the resistive torque (Figure 4(b)-(f)). Figure 5 demonstrates the manner the system can act with an instant reverse speed (Figure 5(a)). The proposed scheme maintains high performance even when reversing the direction of rotation. Strong torque is noticed at the time of the transition of the reference, this high value of approximately -17 $N.m$ is a reaction of the VC to keep the fast pursuit (Figure 5(b)-(f)). In Figures 6(a)-(f) and 7(a)-(f), the good performance of high and low-speed tracking is obtained with less static error. The system keeps the good tracking of the speed, and the torque is responding accordingly with the speed reference.

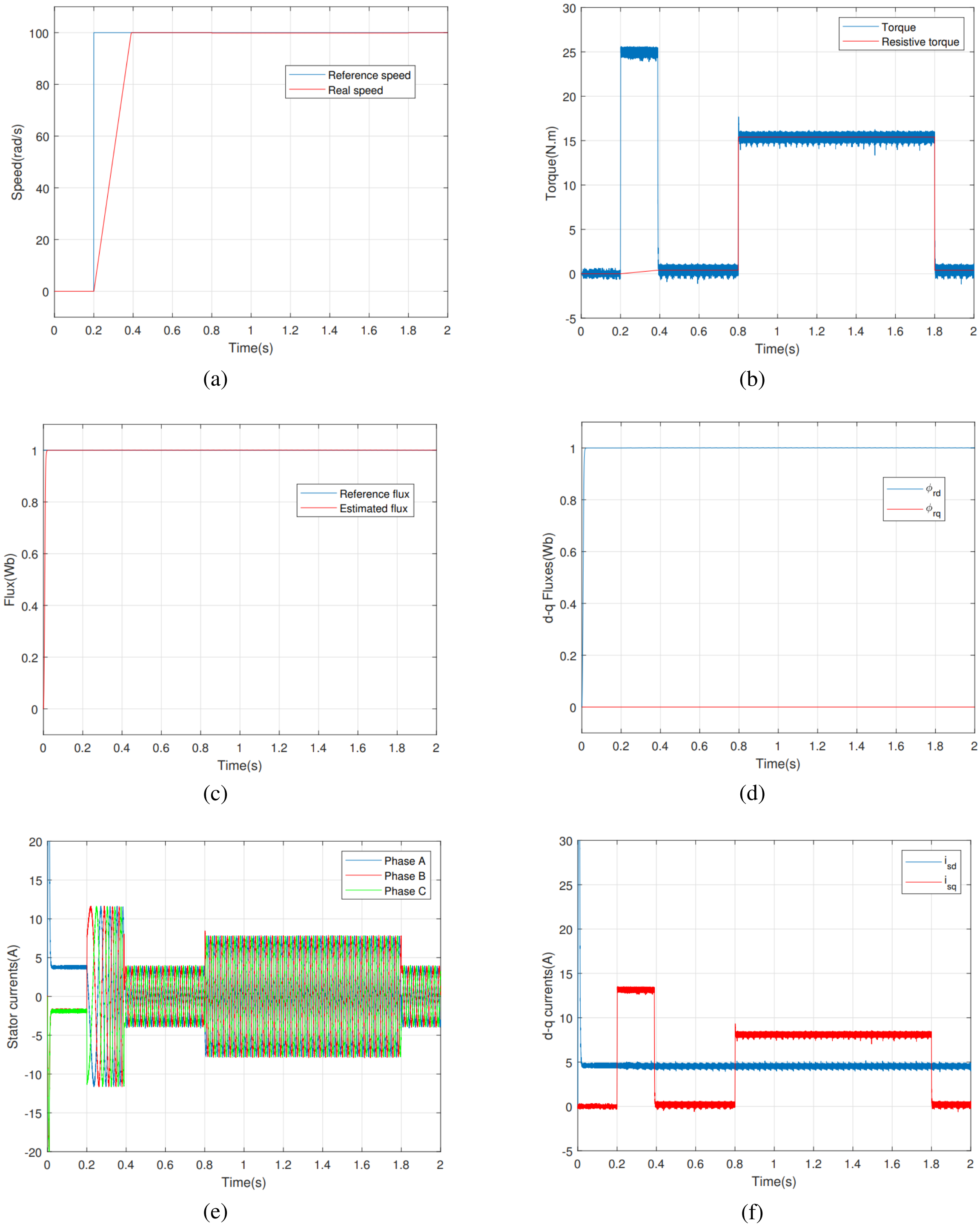

Figure 4. Load torque operation (a) mechanical speed, (b) electromagnetic torque, (c) rotor flux, (d) d-q flux components, (e) phase currents and (f) d-q current components

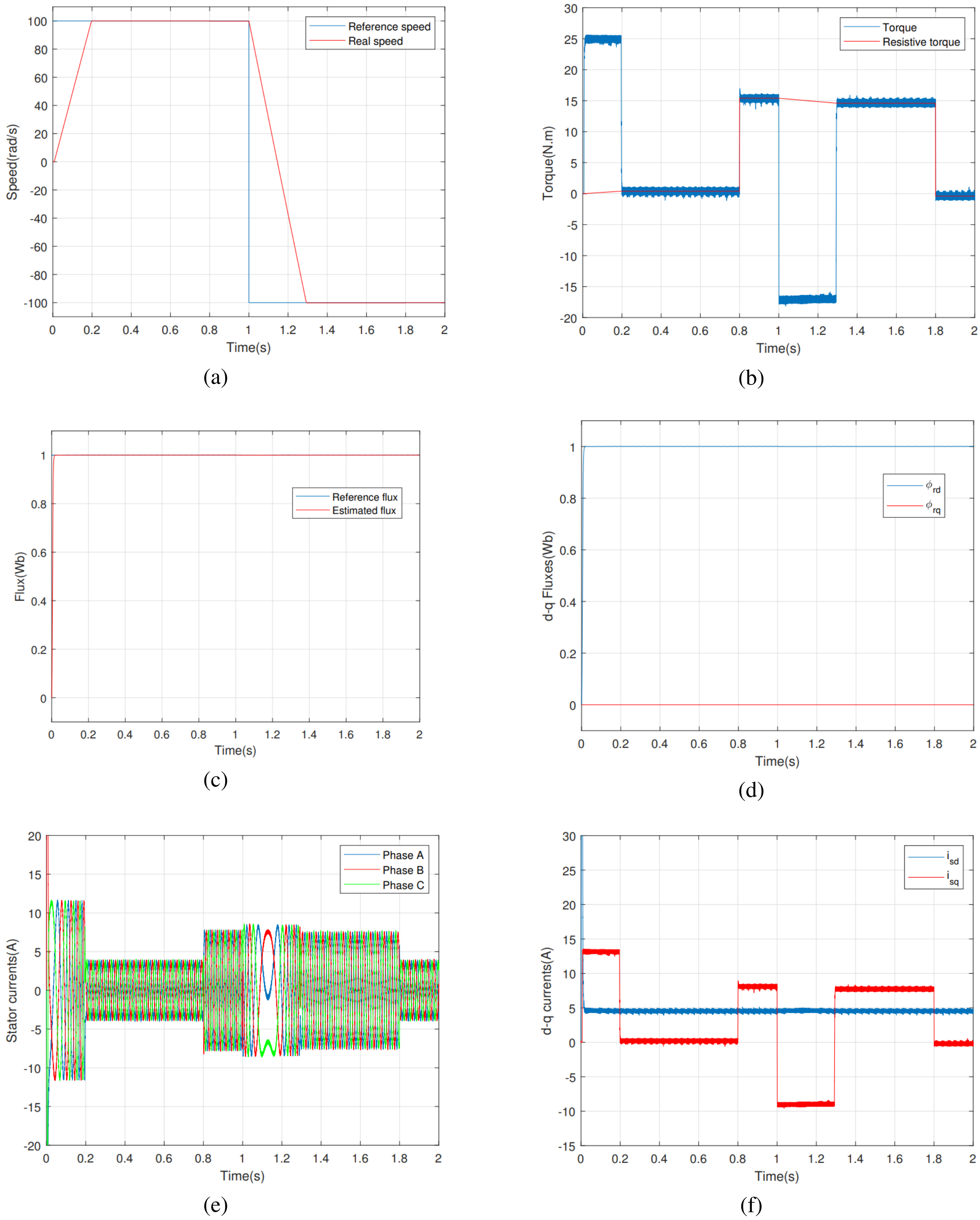

Figure 5. Test with reverse speed (a) mechanical speed, (b) electromagnetic torque, (c) rotor flux, (d) *d*-*q* flux components, (e) phase currents and (f) *d*-*q* current components

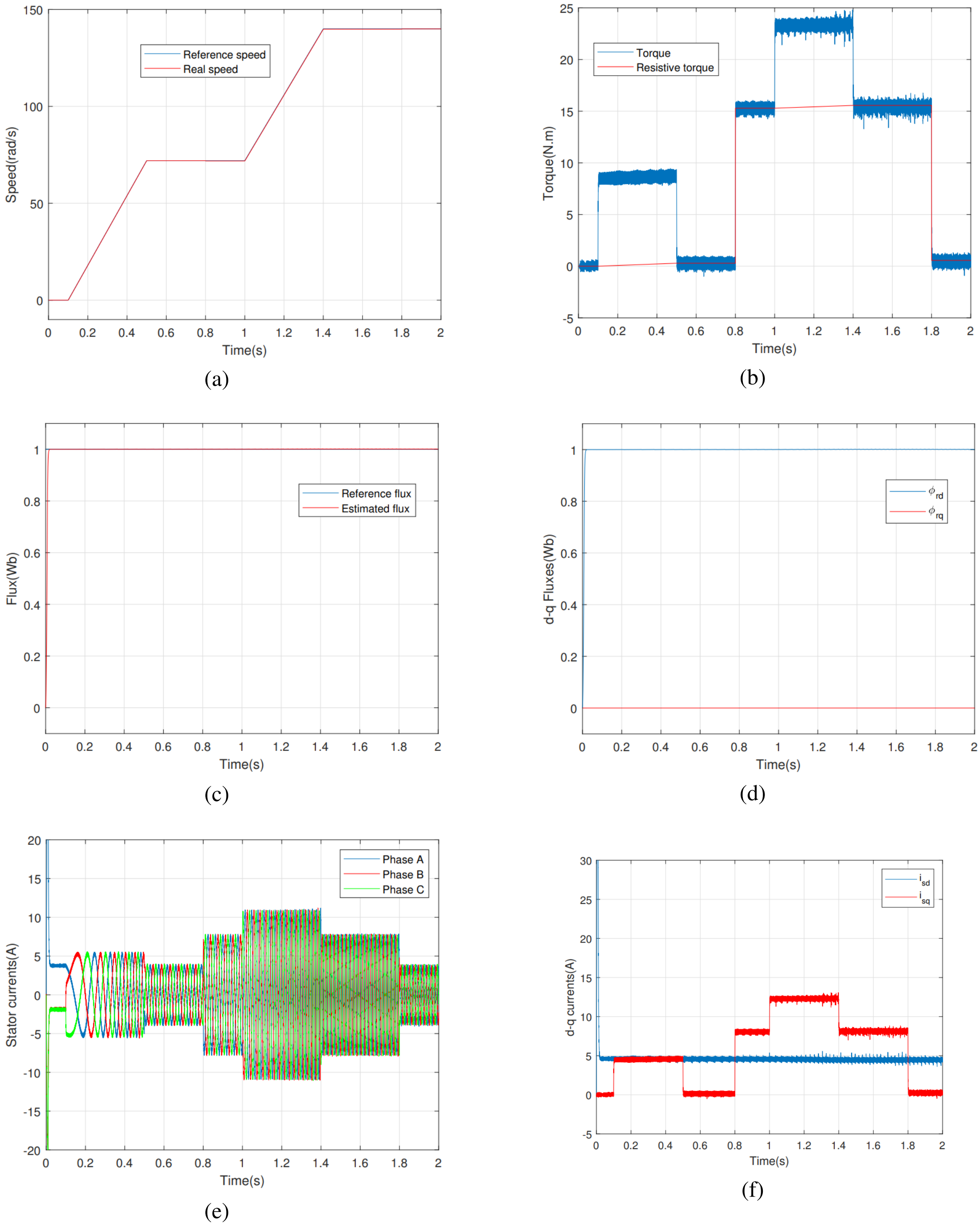

Figure 6. High-speed operation (a) mechanical speed, (b) electromagnetic torque, (c) rotor flux, (d) *d*-*q* flux components, (e) phase currents and (f) *d*-*q* current components

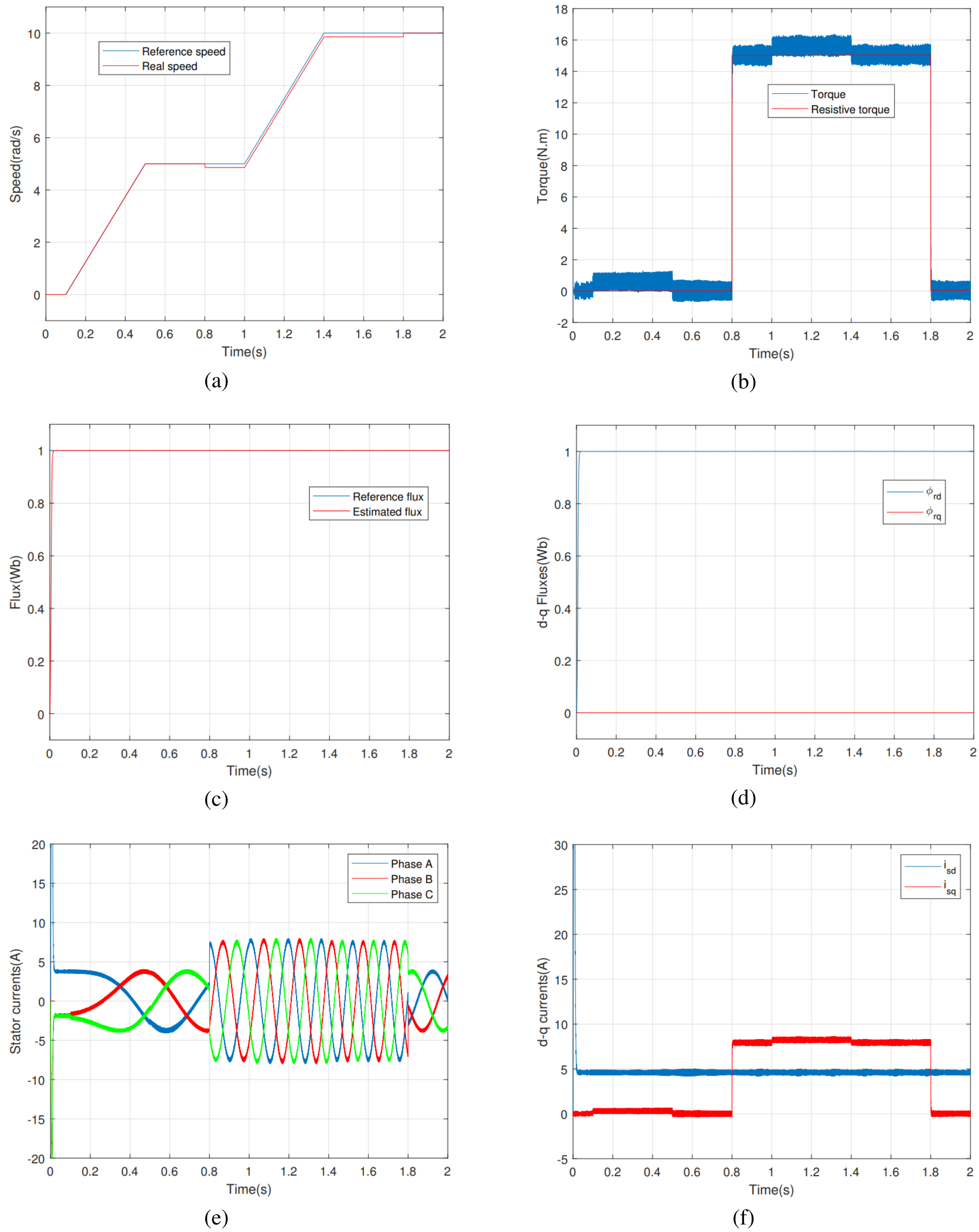

Figure 7. Low-speed operation (a) mechanical speed, (b) electromagnetic torque, (c) rotor flux, (d) *d*-*q* flux components, (e) phase currents and (f) *d*-*q* current components

7. CONCLUSION

In this paper, the operation of the VC-based five-level topology that appealed to the induction motor (IM) has been elaborated on and simulated. The attained results have affirmed the effectiveness and the accuracy of the suggested control scheme over sudden resistive torque, reversal, and high and low-speed regions. The proposed technique ensures better control and robustness; the wrench is the five-level NPC inverter that generates a wide interval of the voltage control sequence. Besides, the SMC ensure high resistance toward the instant load application. Satisfactory results have been obtained by numerical simulation, and a detailed discussion has been presented. Multilevel inverters base generally on symmetrical triangle carriers. Their arrangement characterizes the modulation method. The combination of the comparison signals determines the modulated signal and hence directs the control signals. Four alternate carriers are utilized by the PWM unit to control the five-level inverter switches. The alternate carriers have the advantage of allowing sampling at twice the carrier frequency, which results in a signal that is generally of better quality.

ACKNOWLEDGEMENT

The authors would like to thank the Ph.D. students and professors of the "Laboratoire d'Électronique de Puissance et Commande (EPC) de l'École Mohammadia d'Ingénieurs (EMI)" for their valuable remarks and proposals.

REFERENCES

[1] C. Fahassa, Y. Sayouti, and M. Akherraz, "Improvement of the induction motor drive's indirect field oriented control performance by substituting its speed and current controllers with fuzzy logic components," in *2015 3rd International Renewable and Sustainable Energy Conference (IRSEC)*, Dec. 2015, doi: 10.1109/irsec.2015.7454928.

[2] H. Heidari *et al.*, "A Novel Vector Control Strategy for a Six-Phase Induction Motor with Low Torque Ripples and Harmonic Currents," *Energies*, vol. 12, no. 6, p. 1102, Mar. 2019, doi: 10.3390/en12061102.

[3] U. Syamkumar and B. Jayanand, "Real-time implementation of sensorless indirect field-oriented control of three-phase induction motor using a Kalman smoothing-based observer," *International Transactions on Electrical Energy Systems*, vol. 30, no. 2, Nov. 2019, doi: 10.1002/2050-7038.12242.

[4] H. Dahmardeh, M. Ghanbari, and S. M. Rakhtala, "A Novel Combined DTC Method and SFOC System for Three-phase Induction Machine Drives with PWM Switching Method," *Journal of Operation and Automation in Power Engineering*, vol. 11, no. 2, pp. 76–82, Aug. 2023, doi: 10.22098/joape.2023.9717.1679.

[5] M. Z. Ali, M. N. S. K. Shabbir, S. M. K. Zaman, and X. Liang, "Single- and Multi-Fault Diagnosis Using Machine Learning for Variable Frequency Drive-Fed Induction Motors," *IEEE Transactions on Industry Applications*, vol. 56, no. 3, pp. 2324–2337, May 2020, doi: 10.1109/tia.2020.2974151.

[6] Y. Zahraoui, M. Akherraz, C. Fahassa, and S. Elbadaoui, "Induction motor harmonic reduction using space vector modulation algorithm," *Bulletin of Electrical Engineering and Informatics*, vol. 9, no. 2, pp. 452–465, Apr. 2020, doi: 10.11591/eei.v9i2.1682.

[7] C. Laoufi, Z. Sadoune, A. Abbou, and M. Akherraz, "New model of electric traction drive based sliding mode controller in field-oriented control of induction motor fed by multilevel inverter," *International Journal of Power Electronics and Drive Systems (IJPEDS)*, vol. 11, no. 1, p. 242, Mar. 2020, doi: 10.11591/ijpeds.v11.i1.pp242-250.

[8] B. N. C. V. Chakravarthi, P. Naveen, S. Pragaspathy, and V. S. N. N. Raju, "Performance of Induction Motor with hybrid Multi level inverter for Electric vehicles," in *2021 International Conference on Artificial Intelligence and Smart Systems (ICAIS)*, Mar. 2021, doi: 10.1109/icais50930.2021.9395885.

[9] G. K. Srinivasan, M. Rivera, V. Loganathan, D. Ravikumar, and B. Mohan, "Trends and Challenges in Multi-Level Inverter with Reduced Switches," *Electronics*, vol. 10, no. 4, p. 368, Feb. 2021, doi: 10.3390/electronics10040368.

[10] C. Fahassa, Y. Zahraoui, M. Akherraz, and A. Bennassar, "Improvement of induction motor performance at low speeds using fuzzy logic adaptation mechanism based sensorless direct field oriented control and fuzzy logic controllers (FDFOC)," in *2016 5th International Conference on Multimedia Computing and Systems (ICMCS)*, Sep. 2016, doi: 10.1109/icmcs.2016.7905545.

[11] P. Omer, J. Kumar, and B. S. Surjan, "A Review on Reduced Switch Count Multilevel Inverter Topologies," *IEEE Access*, vol. 8, pp. 22281–22302, 2020, doi: 10.1109/access.2020.2969551.

[12] L. Lahcen and B. Bouchiba, "Fuzzy Sliding Mode Controller for Induction Machine Feed by Three Level Inverter," *International Journal of Power Electronics and Drive Systems (IJPEDS)*, vol. 9, no. 1, p. 55, Mar. 2018, doi: 10.11591/ijpeds.v9.i1.pp55-63.

[13] Y. Kali *et al.*, "Current Control of a Six-Phase Induction Machine Drive Based on Discrete-Time Sliding Mode with Time Delay Estimation," *Energies*, vol. 12, no. 1, p. 170, Jan. 2019, doi: 10.3390/en12010170.

[14] Y. Zahraoui, M. Akherraz, C. Fahassa, and S. Elbadaoui, "Robust control of sensorless sliding mode controlled induction motor drive facing a large scale rotor resistance variation," in *Proceedings of the 4th International Conference on Smart City Applications*, Oct. 2019, doi: 10.1145/3368756.3369036.

[15] K. Mohammed, A. Abdelghani, Y. Dris, B. Abdesselam, and H. Mabrouk, "Management power of renewable energy in multiple sources system to feeding the rotor of a doubly-fed induction generator," *Bulletin of Electrical Engineering and Informatics*, vol. 12, no. 2, pp. 619–632, Apr. 2023, doi: 10.11591/eei.v12i2.3885.

[16] M. Boufadene, *Modeling and Control of AC Machine using MATLAB®/SIMULINK*," CRC Press, 2018, doi: 10.1201/9780429029653.

[17] T. X. Nguyen, M. C. H. Nguyen, and C. D. Tran, "Sensor fault diagnosis technique applied to three-phase induction motor drive," *Bulletin of Electrical Engineering and Informatics*, vol. 11, no. 6, pp. 3127–3135, Dec. 2022, doi: 10.11591/eei.v11i6.4253.

[18] J. Tang, Y. Yang, F. Blaabjerg, J. Chen, L. Diao, and Z. Liu, "Parameter Identification of Inverter-Fed Induction Motors: A Review," *Energies*, vol. 11, no. 9, p. 2194, Aug. 2018, doi: 10.3390/en11092194.

[19] K. Wang, Y. Li, Q. Ge, and L. Shi, "An Improved Indirect Field-Oriented Control Scheme for Linear Induction Motor Traction Drives," *IEEE Transactions on Industrial Electronics*, vol. 65, no. 12, pp. 9928–9937, Dec. 2018, doi: 10.1109/tie.2018.2815940.

[20] X. Zhang, B. Wang, Y. Yu, J. Zhang, J. Dong, and D. Xu, "Analysis and Optimization of Current Dynamic Control in Induction Motor Field-Weakening Region," *IEEE Transactions on Power Electronics*, vol. 35, no. 9, pp. 8860–8866, Sep. 2020, doi: 10.1109/tpel.2020.2968978.

[21] M. A. Hannan, J. A. Ali, A. Mohamed, and A. Hussain, "Optimization techniques to enhance the performance of induction motor drives: A review," *Renewable and Sustainable Energy Reviews*, vol. 81, pp. 1611–1626, Jan. 2018, doi: 10.1016/j.rser.2017.05.240.

[22] F. Wang, Z. Zhang, X. Mei, J. Rodríguez, and R. Kennel, "Advanced Control Strategies of Induction Machine: Field Oriented Control, Direct Torque Control and Model Predictive Control," *Energies*, vol. 11, no. 1, p. 120, Jan. 2018, doi: 10.3390/en11010120.

[23] T. D. Do, N. D. Le, V. H. Phuong, and N. T. Lam, "Implementation of FOC algorithm using FPGA for GaN-based three phase induction motor drive," *Bulletin of Electrical Engineering and Informatics*, vol. 11, no. 2, pp. 636–645, Apr. 2022, doi: 10.11591/eei.v11i2.3569.

[24] Z. Yang, Q. Ding, X. Sun, H. Zhu, and C. Lu, "Fractional-order sliding mode control for a bearingless induction motor based on improved load torque observer," *Journal of the Franklin Institute*, vol. 358, no. 7, pp. 3701–3725, May 2021, doi: 10.1016/j.jfranklin.2021.03.006.

[25] F. M. Zaihidee, S. Mekhilef, and M. Mubin, "Robust Speed Control of PMSM Using Sliding Mode Control (SMC)—A Review," *Energies*, vol. 12, no. 9, p. 1669, May 2019, doi: 10.3390/en12091669.

[26] A. Devanshu, M. Singh, and N. Kumar, "Sliding Mode Control of Induction Motor Drive Based on Feedback Linearization," *IETE Journal of Research*, vol. 66, no. 2, pp. 256–269, Jun. 2018, doi: 10.1080/03772063.2018.1486743.

[27] P. Ramasamy and V. Krishnasamy, "SVPWM control strategy for a three phase five level dual inverter fed open-end winding induction motor," *ISA Transactions*, vol. 102, pp. 105–116, Jul. 2020, doi: 10.1016/j.isatra.2020.02.034.

[28] O. C. Sekhar and S. Lakhimsetty, "Direct torque control scheme for a five-level multipoint clamped inverter fed induction motor drive using fractional-order PI controller," *International Transactions on Electrical Energy Systems*, vol. 30, no. 9, May 2020, doi: 10.1002/2050-7038.12474.

[29] A. Kersten, E. Grunditz, and T. Thiringer, "Efficiency of Active Three-Level and Five-Level NPC Inverters Compared to a Two-Level Inverter in a Vehicle," in *2018 20th European Conference on Power Electronics and Applications (EPE'18 ECCE Europe)*, Riga, Latvia, Sep. 2018, p. P.1-P.9.

[30] K. D. Pham, Q. V. Nguyen, and N.-V. Nguyen, "PWM Strategy to Alleviate Common-Mode Voltage with Minimized Output Harmonic Distortion for Five-Level Cascaded H-Bridge Converters," *Energies*, vol. 14, no. 15, p. 4476, Jul. 2021, doi: 10.3390/en14154476.

BIOGRAPHIES OF AUTHORS

Chaymae Fahassa received an Engineer's Degree in Mechatronics from the Abdelmalek Essaadi University of Tetouan in 2012. Currently, she is a Ph.D. student in Electrical Engineering in the Laboratory of Power Electronics and Control (PEC) from Mohammed V University, Mohammadia School of Engineering. Her research interests concern AC motors control using artificial intelligence, especially induction motors, sensorless control techniques, hybrid control strategies, power electronics, and renewable energy sources. She can be contacted at email: fahassa.chaymae@gmail.com.

Ahmed Abbou received the B.E. degree from ENSET in Rabat, the M.E. degree from Mohammed V University in Rabat and the Ph.D. degree from Mohammed V University in Rabat, in 2000, 2005 and 2009, respectively, all in Electrical Engineering. Since 2009, he has been working at Mohammadia School of Engineering, Mohammed V University in Rabat, Department of Electric Power Engineering, where he is a full Professor of Power Electronics and Electric Drives. He published numerous papers in scientific international journals and conference proceedings. His current research interests include induction machine control systems, self-excited induction generator, power electronics, sensorless drives for AC machines and renewable energy (PV and wind energy). He can be contacted at email: abbou@emi.ac.ma.

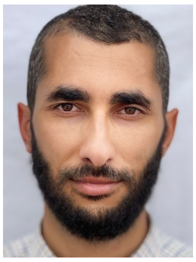

Yassine Zahraoui learned a Master's degree in Data Processing from Hassan II University, Casablanca in 2011. He received his Ph.D. degree in Electrical Engineering from Mohammed V University, Mohammadia School of Engineering, Rabat in 2021. He is currently a Ph.D. student for a second thesis at the University of Hassan II, Higher National School of Arts and Crafts, Casablanca. He published many papers in scientific international journals and conference proceedings, and he is a reviewer for many highly indexed journals. His research interests include the AC drives robust and sensorless control strategies, especially synchronous reluctance and induction motors. The main research focuses on ripple reduction and performance improvement. Future prospects are focused on electric cars and renewable and sustainable energy sources. He can be contacted at email: yassine.zahraoui1-etu@etu.univh2c.ma.

Mohamed Akherraz graduated from the Mohammadia School of Engineering in Rabat, Morocco. He graduated with a Fulbright scholarship to pursue his post-graduate studies. He received his Ph.D. degree in 1987 from UW, Seattle. He joined the Electrical Engineering Department of the Mohammadia School of Engineering, Rabat where he is currently a Professor of Power Electronics and Electric Drives. He published numerous papers in scientific international journals and conference proceedings. His areas of interest are power electronics, electric drives, computer modeling of power electronics circuits, and system drives. He can be contacted at email: akherraz@emi.ac.ma.